Adsorption of Zein on Surfaces with Controlled Wettability and Thermal Stability of Adsorbed Zein Films

S. Subramanian and S. Sampath*

Department of Inorganic and Physical Chemistry, Indian Institute of Science, Bangalore 560 012, India

Received February 17, 2007; Revised Manuscript Received April 20, 2007

Adsorption characteristics of zein protein on hydrophobic and hydrophilic surfaces have been investigated to understand the orientation changes associated with the protein structure on a surface. The protein is adsorbed by a self-assembly procedure on a monolayer-modified gold surface. It is observed that zein shows higher affinity toward hydrophilic than hydrophobic surfaces on the basis of the initial adsorption rate followed by quartz crystal microbalance studies. Reflection absorption infrared (RAIR) spectroscopic studies reveal the orientation changes associated with the adsorbed zein films. Upon adsorption, the protein is found to be denatured and the transformation of α-helix to β-sheet form is inferred. This transformation is pronounced when the protein is adsorbed on hydrophobic surfaces as compared to hydrophilic surfaces. Electrochemical techniques (cyclic voltammetry and impedance techniques) are very useful in assessing the permeability of zein film. It is observed that the zein moieties adsorbed on hydrophilic surfaces are highly impermeable in nature and act as a barrier for small molecules. The topographical features of the deposits before and after adsorption are analyzed by atomic force microscopy. The protein adsorbed on hydrophilic surface shows rod- and disclike features that are likely to be the base units for the growth of cylindrical structures of zein. The thermal stability of the adsorbed zein film has been followed by variable-temperature RAIR measurements.

Introduction

Enzymes and proteins often show specific adsorption on surfaces, and the interactions are generally governed by charge-based and hydrophobic forces.[1] Nonspecific interactions involving proteins are of interest in applications such as immunoassays,[2] biofouling,[3] and biocompatibility.[4] Adsorption characteristics of proteins and enzymes are fundamentally important to appreciate relaxation characteristics, unfolding, footprint, and coverage.[5−7] Additionally, protein molecules having hydrophilic and hydrophobic moieties may change their conformation upon adsorption on surfaces of different wettablity.[1,5] The mechanism of adsorption of globular proteins at solid/water interfaces has been reported in detail.[8,9]

Cereal proteins are used as encapsulates for food,[10] oils,[11] and extruded products by plasticizing with fatty acids or lipids.[12] Zein is a prolamine of maize and it has attracted attention because of its potential applications as an industrial biopolymer.[13] Zein is classified as a globular protein containing a large fraction of nonpolar amino acids.[14] The structure of zein as reported by Matsushima et al.,[15] based on small-angle X-ray scattering (SAXS), contains 10 successive helical segments folded upon each other in an antiparallel fashion stabilized by hydrogen bonds. The helical segments are linked at each end by glutamine-rich turns or loops (Scheme 1). Zein has been used to produce novel polymeric films that are biodegradable[13] and can be used as a coating to protect food materials from spoilage.[10] Zein films can replace commercial coating agents like carnauba wax and shellac inside food packets. The properties of the films, like biodegradability, mechanical properties, water absorption and barrier properties, etc., largely depend on the interaction between proteins, plasticizers, and other functional groups,[16] and monolayers are good models to study their properties.[17]

Scheme 1. Structure of Zein Monomer (after Reference 15)

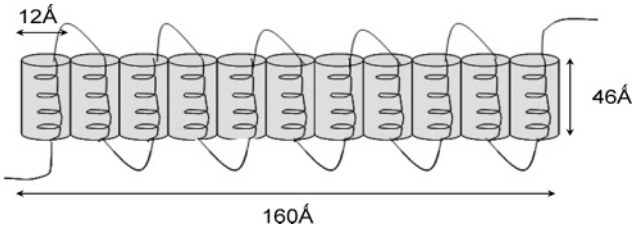

Spectroscopic studies on the zein films concerning stability, degradability, and interactions with plasticizers have been reported earlier.[18,19] Fourier transform infrared spectroscopy (FT-IR)[20] and Raman spectroscopy[21] have been used extensively to follow conformational changes associated with zein films. Raman spectroscopic studies on zein films have been reported to monitor the thickness and evaluate the ability of the film performance as a food-protecting agent.[22] Zein protein is neither soluble in pure water nor in alcohol since it contains both hydrophilic and hydrophobic character according to the model proposed by Matsushima et al.[15] The average hydrophobicity of zein is reported to be 50 times larger than albumin, fibrinogen, etc., and hence a higher percentage of alcohol/aqueous mixture is required for dispersion of zein.[23] The solvent that is used in the present study is 75% (by volume) 2-propanol in water as reported in the literature.[23]

It is important to understand the characteristics of adsorbed zein film in terms of its permeability to small molecules, since this biopolymer is projected to be a good coating material for food packaging. Additionally, the hydrophilic and hydrophobic residues on the protein surface may play a large role in determining the orientation of the protein when adsorbed on surfaces with controlled wettability. The change in orientation is expected to result in surfaces with controlled characteristics that could be used for a variety of applications. In the present study, we have adsorbed zein on hydrophilic and hydrophobic

* Author to whom correspondence should be addressed. E-mail: sampath@ipc.iisc.ernet.in.

10.1021/bm0701999 CCC: $37.00
Published on Web 06/14/2007

surfaces and show that the permeability of the film varies depending on the orientation of the protein on the surface. The importance of interactions of zein with polar and nonpolar functional groups is brought out in the context of fatty acids and lipids being used for making biopolymer films of zein for industrial applications. This information may prove to be very useful in the fabrication of zein films toward biodegradable, edible, preservative coatings for food materials. A variety of techniques including quartz crystal microbalance (QCM), reflection absorption infrared (RAIR), atomic force microscopy (AFM), and electrochemical techniques[24,25] have been used to understand the adsorption behavior of zein. Thermal stability and orientation changes associated with zein deposits have been monitored by RAIR spectroscopy based on the changes associated with the amide stretching modes.

Experimental Section

Chemicals. Mercaptoundecanoic acid [$SH(CH_2)_{11}COOH$, 99.98%, Aldrich] and undecanethiol [$CH_3(CH_2)_{10}SH$, 99.98%, Aldrich] were purchased and used without further purification. Potassium ferricyanide (99.9%), potassium ferrocyanide (99.9%, SD Fine Chemicals), sodium fluoride (99.8%, Merck), ethanol (99.99%), 2-propanol (99%, SD Fine Chemicals) were used as received. Zein (from maize) was purchased from Sigma and defatted by the procedure given below. Double-distilled water was used wherever required.

Purification of Zein. Commercial zein was defatted with hexane, on the basis of a reported procedure.[26] A definite volume of ethanolic solution of zein was kept in a rotary evaporator until all the ethanol was evaporated. A known volume of HPLC-grade hexane was then added to it, the mixture was filtered, and the remaining hexane was evaporated in a rotary evaporator. This process was repeated at least three times till no fat was detected in the filtrate.

To check the purity of defatted zein, sodium dodecyl sulfate−polyacrylamide gel electrophoresis (SDS−PAGE) was carried out in an SDS−12% polyacrylamide gel. Buffer containing 49 mM Tris, 384 mM glycine, and 0.1% (w/v) SDS at pH 8.5 was used to run the gel electrophoresis. Coomassie blue staining was used for detection of polypeptides. Molecular masses of SDS−PAGE standards ranged from 10 to 90 kDa.

Substrate Preparation. Highly oriented (111) gold surface was prepared by resistive thermal evaporation of gold (1500−2000 Å thickness) on fine-quality mica sheets. The powder XRD data confirmed the formation of oriented (111) phase. The roughness factor defined as the ratio of the real surface area to the geometric area of the Au surface was determined to be 1.5 for the as-deposited gold, based on oxide stripping in 0.5 M H_2SO_4. The gold surfaces were flame-annealed in an acetylene−oxygen flame and subsequently washed with ethanol before use.

Monolayer Formation: *Adsorption of Carboxyl-Terminated Self-Assembled Monolayers.* Hydrophilic surfaces were prepared by adsorption of mercaptoundecanoic acid (MuDA) on oriented gold surfaces. The gold substrates were immersed in 1 mM solution of mercaptoundecanoic acid in ethanol for 12 h and subsequently washed with a copious amount of solvent. The modified surfaces were dried in argon and used for further studies.

Adsorption of Methyl-Terminated Self-Assembled Monolayers. Hydrophobic surfaces were prepared by adsorption of undecanethiol on gold surfaces. Gold substrates were immersed in 1 mM solution of undecanethiol in ethanol for 12 h and subsequently rinsed with alcohol and dried in argon gas.

Zein Adsorption on Modified Substrates. The self-assembled monolayer- (SAM-) modified gold surfaces were immersed in 0.05% (w/v) zein in 2-propanol−water (3:1 by volume) mixture for 2 h and subsequently rinsed with the solvent to remove loosely bound zein molecules. In the case of zein adsorption on carboxylic acid-terminated SAM, the pH of the aqueous phase used to prepare the solvent for zein is adjusted to pH = 4 with chloroacetic acid. At this acidic pH, it is expected that the carboxylic acid functional groups of the SAM will be in the undissociated form. The interaction of the carboxylic acid end groups with the glutamine residues of zein may thus be favored. Though it is not truly a hydrophilic−hydrophilic interaction as in an aqueous medium, it is expected that the COOH groups will interact with the glutamine residues in the mixed solvent of water−2-propanol.

Reflection Absorption Infrared Spectroscopy. RAIR spectra were recorded on a FT-IR spectrometer (Spectrum GX, Perkin-Elmer, Switzerland) equipped with a liquid nitrogen-cooled HgCdTe (MCT) detector. The p-polarized infrared beam was reflected from the SAM-modified surface at an angle of 75° to the surface normal. The spectra were generally averaged over 1024 scans with a resolution of 4 cm^{-1} and referenced to bare gold substrates. The variable-temperature measurements were carried out in situ with a high-temperature accessory (Harrick). The high-temperature accessory is a reactor used for high-temperature IR measurements and is combined with a Perkin-Elmer IR spectrometer. The accessory allows us to perform IR measurements at high temperatures (400 °C) as well as at a pressure of 2 atm. The sample is heated at 1 °C/min in a closed chamber with heating leads at three different ends of the sample plate. The sample size is about 3 cm × 1 cm. This is kept at the desired temperature for several minutes before the spectrum is recorded. A heating pad spread over the entire base is used to ensure uniform heating of the sample. Prior to the experiment, the sample chamber and heating accessory was purged with ultra-high-purity argon gas to maintain an inert atmosphere. The IR spectral analysis was carried out with Spectrum 3.02 version (Perkin-Elmer) software as well as Microcal Origin 6.0 software for data analysis (Version 6.1052, Origin Lab Corp.).

Quartz Crystal Microbalance Studies. QCM is a powerful technique to understand the adsorption behavior of organic molecules, proteins, and other biomolecules on various substrates.[24] Adsorption characteristics like rate of adsorption, thickness of the film, and number of molecules can be obtained from the frequency changes observed during the adsorption process.[24] The quartz crystal microbalance measurements were carried out on a CHI400 EQCM. Quartz crystal covered with gold sputtered on a Ti layer with a 7.995 MHz fundamental frequency was used as the working electrode. The electrodes were cleaned by rinsing with deionized water and kept in ethanol for 10 min prior to use.

Atomic Force Microscopy. Atomic force microscopy (AFM) measurements were carried out on a CP-II scanning probe microscope (Thermomicroscopes). Silicon nitride probes coated with gold on one side, having a spring constant of 0.1 N/m, were used. Topographical features were obtained by contact mode imaging with 3 μm × 3 μm scale, and Proscan 1.7 version software was used for the analysis.

Electrochemical Studies. All the electrochemical studies were carried out with a three-electrode setup, with modified gold as the working electrode, platinum foil as the counterelectrode, and saturated calomel as the reference electrode. Cyclic voltammetry measurements were carried out at a scan rate of 0.05 V/s in the potential range of −0.2 to 0.4 V in the presence of 0.1 M NaF as the supporting electrolyte under inert atmosphere. Electrochemical accessibility studies were carried out with 3 mM potassium ferrocyanide/3 mM potassium ferricyanide in 0.1 M NaF. Impedance spectra were collected in the frequency range of 100 kHz−100 mHz (Model 5210, EG&G Parc) with 5 mV rms ac perturbation at 0.2 V DC bias.

Results and Discussion

The electrophoretic profiles of defatted zein at two different concentrations show bands around 17 kDa, revealing that a large percentage of the sample is in the α form. This agrees with the previous reports[15,27] on molecular weight distribution of commercial zein samples.

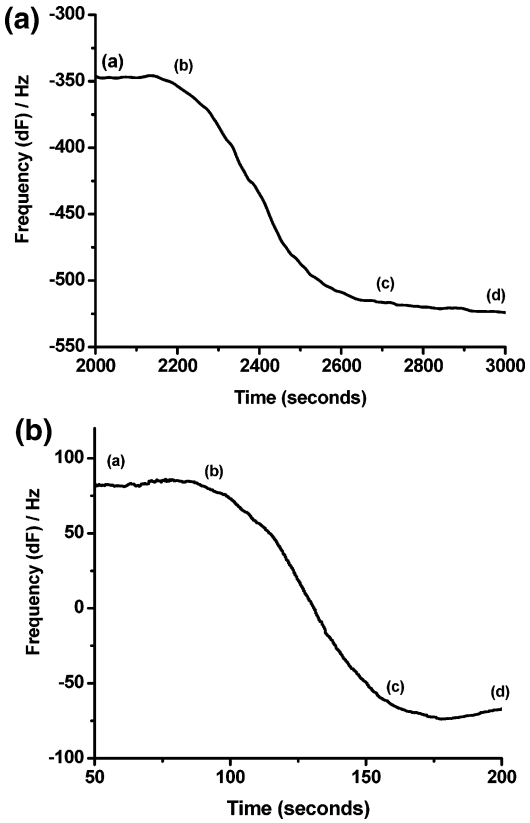

Figure 1. (Top panel) Frequency variation with time for zein deposition on hydrophobic surfaces (undecanethiol SAM-modified surfaces). Labels a−d are described in the text. The *y*-axis shows the frequency change with respect to the fundamental frequency of the crystal as the starting point. The frequency decrease associated with increased mass is shown as the negative change in adsorption. The *x*-axis shows the time scale associated with stabilization of frequency as the starting point, before zein is injected. (Bottom panel) Frequency variation with time for zein deposition on hydrophilic surfaces (mercaptoundecanoicacid SAM-modified surfaces). Labels a−d are described in the text. The *y*-axis shows the frequency change with respect to fundamental frequency of the crystal as the starting point. The frequency decrease associated with increased mass is shown as the negative change in adsorption. The *x*-axis shows the time scale associated with stabilization of frequency as the starting point, before zein is injected.

Quartz Crystal Microbalance Studies. The adsorption characteristics of zein protein on hydrophilic and hydrophobic substrates have been followed by QCM. Quartz resonators coated with gold have been modified with undecanethiol and 11-mercaptoundecanoic acid and used as substrates for further adsorption of zein. Figure 1 (top) shows the frequency change observed during the adsorption of zein on hydrophobic surface as a function of time. Initially the QCM frequency is stabilized in presence of the solvent that is shown by the region a−b in the figure. At point b, zein solution (0.05 w/v) in 2-propanol−water mixture (3:1 by volume) is injected and the frequency starts to decrease monotonically, as indicated by the region b−c. The stable frequency after point c shows the completion of adsorption. The frequency change can be correlated to the mass change by use of the Saurbery equation. This relates the mass change associated with the frequency change of a quartz crystal resonator in the fundamental vibration mode. This equation can be represented as

$$\Delta f = -(2f_0^2/A\sqrt{\mu\rho})\,\Delta m = -C_f \Delta m$$

where Δf (hertz) is the frequency change observed on adsorption, Δm is the mass change, f_0 is the fundamental resonant frequency of the crystal, A the area of the gold deposited on quartz, ρ is the density of the crystal, and μ is the shear modulus of quartz. All the parameters except Δm are constant for a given environment and can be denoted as C_f, the proportionality constant. In the present study, the constant is observed to be 0.14 ng for a frequency change of 0.1 Hz. The frequency change corresponding to the zein adsorption is observed to be 170 Hz. This corresponds to the mass of adsorbed zein as 645.5 ng/cm^2 (after correcting for real surface area of the Au surface) calculated on the basis of the Sauerbery equation.[28]

Similarly, the frequency change for zein adsorption on hydrophilic surfaces (MuDA SAMs; Figure 1, bottom) is observed to be 165 Hz, which corresponds to a mass of 1033 ng/cm^2. Though the frequency variation is similar, the mass adsorbed is different due to different roughness associated with the gold surfaces. The hydrophilic surfaces show higher coverage than hydrophobic surfaces. The time scale associated with the adsorption shows zein's affinity toward hydrophilic surfaces as compared to hydrophobic surfaces. The coverage determined indicates that the protein possibly adopts different orientations, resulting in different mass changes observed in the QCM measurements. It should however, be pointed out that stronger protein−surface interactions leading to denaturation of the protein might result in low coverage. In the present studies, denaturation of the protein occurs irrespective of whether the surface is hydrophilic or hydrophobic, as revealed by the IR spectroscopic studies.

The structure of zein monomer[15] reveals that the size of the helical cylinder responsible for the hydrophobic property is 16 nm × 4.6 nm. On the other hand, glutamine turns connecting the helical structures that are responsible for the polar nature have a size of 16 nm × 1.2 nm. The large footprint size of the hydrophobic moiety hinders the adsorption of the zein monomer with appreciable coverage. This is reflected in rate of adsorption on hydrophobic surface being low as compared to the adsorption on hydrophilic surface. The size of the hydrophilic moiety (smaller footprint size) is small, which makes the interaction facile and hence gives a fast rate of adsorption with high surface coverage. This adsorption kinetics agrees with the reported results based on SPR for zein monolayers on SAMs.[29]

Reflection Absorption Infrared Spectroscopy. The coverage data being different for hydrophilic and hydrophobic surfaces shows that there is a difference in the orientation of zein on the two surfaces. The noninvasive RAIRS technique provides a direct method to understand the local information on protein secondary structure and its arrangement of side groups like tryptophan, tyrosine, phenylalanine, and other residues.[18,20,21,30] The band assignments are carried out based on previous studies on zein films by FT-IR spectroscopy.[18,20,21,30] The FT-IR spectrum of bulk zein in the transmittance mode is given in the Supporting Information. Characteristic bands at 3308, 1660, 1535, 1447, 1238, and 700 cm^{-1} (Table 1)[30] show the presence of zein predominantly in the α-helix structure. The broad nature amide I band shows the presence of other conformers like α-helix, β-sheet, β-turns, and β-sheet with intermolecular hydrogen bonding present in small fractions.[20,21] The following discussion based on amide bands gives clear information on conformational changes of protein molecules on the different substrates.

Hydrophobic Surfaces. The RAIR spectrum of zein film on a hydrophobic surface is given in Figure 2 (left side, spectrum i). The bands at 3271 and 1622 cm^{-1} (amide I) are assigned to N−H stretching and C═O stretching of the amide group. The

Table 1. IR Bands and Corresponding Assignments for Zein Films[a]

origin	wavelength (cm^{-1})	assignment
amine	3308	N−H stretching
amide I	1660	C=O stretching, N−H wagging
amide II	1535	N−H in-plane bend, C−N stretch
aliphatic residues	1447	C−H bending
amide III	1238	N−H in-plane bend, C−N stretch
phenylalanine	997	ring breathing mode
tryptophan	880	indole ring
tyrosine	827	tyrosine residue
amine	700	N−H out-of-plane deformation

[a] Based on refs 21 and 30−32.

N−H out-of-plane deformation observed in the bulk is absent for the film on hydrophobic surfaces. The broad hump around 1536 (amide II) and 1225 cm^{-1} can be assigned to C−N stretching and N−H in-plane deformation[31] modes. Other bands corresponding to C−H vibrations 2920, 2852, and 1436 cm^{-1} and 835, 878, 1020 cm^{-1} (Figure 2, left side, spectrum ii) corresponding to tyrosine, tryptophan, and phenylalanine are also observed in the spectrum.[21]

Amide I Band. The 1600 cm^{-1} region of the RAIR spectrum corresponds to the amide I band for zein. A strong band at 1622 cm^{-1} (Figure 2, left side, spectrum iii) indicates a large amount of β structure in the form of β-sheet conformers associated with the protein.[20] Other conformers like α-helix and β-turns are present and can be inferred from shoulders at 1656 and 1675 cm^{-1} with relatively low intensity. The amide I stretching mode shifting to a low frequency after adsorption clearly indicates the denaturation involving the transformation of α to β structure.[32] It is likely that the interaction of SAMs (methyl-

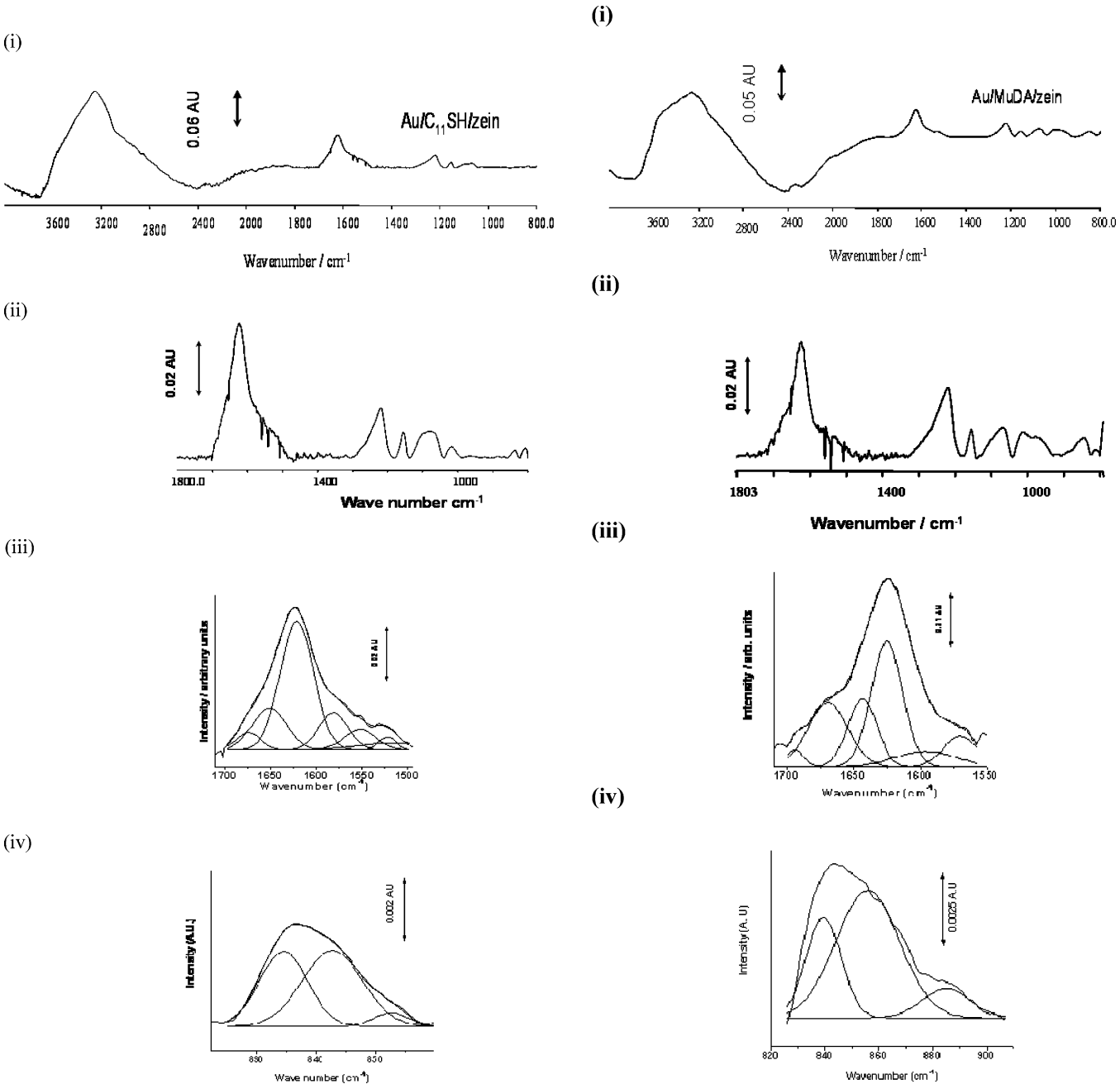

Figure 2. (Left panels) (i) RAIR spectrum of zein film on hydrophobic surface under ambient conditions. (ii) RAIR spectrum in the expanded form (1800−−800 cm^{-1}). (iii, iv) Deconvoluted spectra for amide I and tyrosine bands respectively. (Right panels) RAIR spectrum of film on hydrophilic surface under ambient conditions. (ii) RAIR spectrum in the expanded form (1800−−800 cm^{-1}). (iii, iv) Deconvoluted spectra for amide I and tyrosine bands, respectively.

terminated monolayers) with part of the amino acid residues is responsible for the folding of α-helix. According to the reported structure,[33] the α-helical structure of zein is highly hydrophobic and rich in phenylalanine and tyrosine residues. The methyl group of the SAMs interacts effectively with the residues in the α-helix, which brings down the amount of α-helix conformers. The decrease in α-helix structure is compensated by the increase in β sheet at 1622 cm^{-1}. This effectively buries the tyrosine and phenylalanine residues in the SAM/zein composites. It has been reported that the ratio of intensity of bands at 858 and 835 cm^{-1} is very sensitive to the interaction of tyrosine with nearby groups.[21] An increase in the ratio reveals that the tyrosine residues are on the surface and vice versa. Figure 2 (left side, spectrum iv) shows the RAIR spectrum in the range 800−900 cm^{-1}. The band at 837 cm^{-1} and the shoulder at 856 cm^{-1} correspond to the tyrosine residues, and the ratio of areas of the two bands (856/837) obtained from deconvoluting the spectrum works out to be 0.125. The small value indicates the deeply buried nature of the tyrosine residues in the SAM structure. In other words, the methyl-terminated monolayer penetrates thorough the α-helical structure of the zein and leads to the transformation of α to β structure. On the whole, amide I stretching band implies the denaturation and subsequent transformation of α to β structure.

Amide II Band. The amide II band observed in the RAIR spectrum (bands at 1535 and 1520 cm^{-1}) indicates the presence of α and β structure with substantial amounts of β-sheet conformer. Compared to the bulk spectrum, the band shifts to a low-frequency value, confirming that the proteins are in a denatured state.[32]

Amide III Band. Mizushima and co-workers[35] have reported that the band close to 1250 cm^{-1} is characteristic of the peptide group (amide III band). This band generally splits into a series of components in the region 1220−1350 cm^{-1}, corresponding to different conformers of the protein. The position and the intensity of the band are extremely sensitive to structural changes.[30] In the bulk spectrum of zein (Supporting Information), this band shows a series of peaks at 1238, 1278, 1310, and 1340 cm^{-1}. The band at 1238 cm^{-1} is responsible for the β-structure, while the bands at high wavenumbers correspond to the α-helix. After adsorption of zein protein (Figure 2, left side, spectrum ii), an increase in the intensity of the 1238 cm^{-1} band with a shift from 1238 to 1222 cm^{-1} is observed showing the presence of a substantial amount of β-structure in the zein. The amount of α-helix structure being relatively small can be inferred from the small shoulder at 1272 cm^{-1}.

The above discussion reveals that zein adsorption on hydrophobic surface affects the α-helix structure to a large extent and subsequent transformation to β-sheet structure.

Hydrophilic Surfaces. Figure 2 (right side, spectrum i) shows the RAIR spectrum of zein deposits on hydrophilic surfaces (carboxyl-terminated SAMs). The spectral features are observed to be different from the spectrum observed for zein on hydrophobic surfaces. The amide I band (1624 cm^{-1}) is shifted from the bulk value showing the denaturation of the protein.[32] The shoulders observed at 1677 and 1689 cm^{-1} (Figure 2, right side, spectrum iii) that are absent in the hydrophobic case indicate the amount of α-helix structures being large on the hydrophilic substrate. This reveals that the conformation adopted by the zein molecule is different on the two surfaces. The amide II and III bands reveal the intensity decrease in the β-sheet structure after adsorption. The bands at 840, 868, 974, and 1007 cm^{-1} (Figure 2, right side, spectrum ii) corresponding to free tyrosine, and phenylalanines are clearly observed in the present case. Figure 2 (right side, spectrum iv) shows the RAIR spectrum in range 800−900 cm^{-1}. It is clear that the band at 840 cm^{-1} due to tyrosine residues is broad. The ratio of the areas of the two component observed at 838 and 858 cm^{-1} is 2.3, indicating that the tyrosine residues are present at the surface. Hence, the α-helical structure is preserved and transformation to β structure is not substantial in this case. This supports that the interaction of the SAMs with these residues is not intense and hence the associated bands are not deeply buried inside the zein/SAMs. This is clear evidence for the different interaction modes on the hydrophilic SAMs where the conformation of the protein is different. In this case, the interaction is through the glutamine turns of the zein with the carboxyl group of the SAMs. The absence of a band at 1608 cm^{-1} that is responsible for the scissoring mode of glutamine residues agrees with this argument. Since the interaction is through the glutamine turns that are hydrophilic in nature, the hydrophobic part of zein (the α-helical structure) is not altered in the present case as compared to the hydrophobic surfaces.

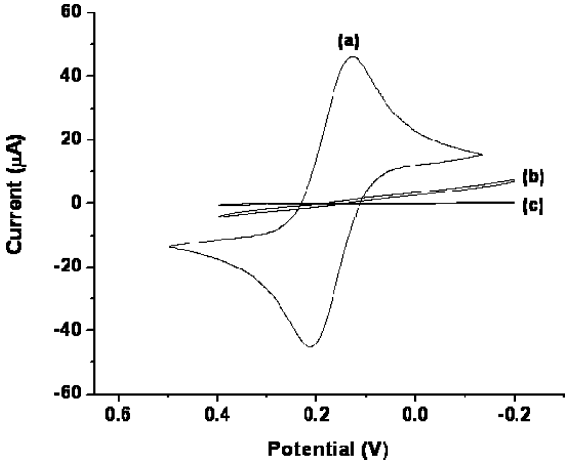

Figure 3. Cyclic voltammograms of 3 mM potassium ferrocyanide/potassium ferricyanide in 0.1 M NaF supporting electrolyte on (a) bare gold surface, (b) zein deposit on hydrophobic monolayer, and (c) zein deposit on hydrophilic monolayer.

Thus, the RAIRS studies bring out the effect of substrate wettability on the conformation adopted by the zein molecule under ambient conditions. Zein when adsorbed on hydrophobic surface experiences a substantial transformation of α-helix structure to β-sheet form, and this transformation is not observed when zein is adsorbed on hydrophilic surfaces.

Electrochemical Characterization. Electrochemical techniques are very effective in assessing the quality of thin films on conducting surfaces.[35−38] The integrity and packing of zein films have been followed using cyclic voltammetry and impedance measurements. Adsorbed zein films on gold surfaces act as a barrier and block the Faradaic process between a diffusing species and the electrode surface. The defects associated with the films can be quantitatively assessed from the current response in the voltammetry by calculating the heterogeneous rate constant associated with the Faradaic process.[39] Figure 3 shows cyclic voltammograms of the modified and unmodified Au electrode in the presence of 3 mM $[Fe(CN)_6]^{4-/3-}$ redox couple in 0.1 M NaF supporting electrolyte. A reversible redox response for the bare Au electrode is clearly observed (Figure 3a). The voltammograms for the zein/SAM-modified electrodes show excellent blocking behavior as revealed by the observed low currents flowing in the cell. The zein-modified surface on a hydrophilic SAM (Figure 3c) shows better blocking behavior than that adsorbed on a hydrophobic surface (Figure 3b),

Table 2. Heterogeneous Electron-Transfer Rate Constant for $[Fe(CN)6]^{3-/4-}$ Couple on Zein Deposits on Modified Monolayers on Gold Surface[a]

temp (°C)	heterogeneous rate constant (cms^{-1}) gold modified with $C_{11}SH$/zein (10^{-4})	gold modified with MuDA/zein (10^{-5})
25	2.3	1.3
35	4.1	1.6
45	3.3	3.2
55	3.1	4.4
65	4.1 (1.2)	5.4 (1.55)
75	5.2 (1.5)	6.3 (1.6)

[a] Rate constants have been calculated on the basis of cyclic voltammetry via the procedure reported by Krysinski and Smolska.[40] Values in parentheses are calculated at room temperature after the system is cooled from the corresponding high temperature.

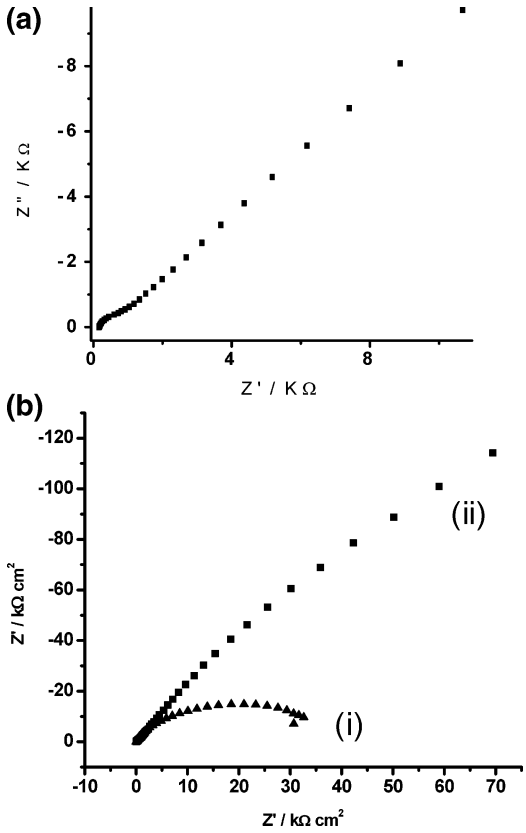

Figure 4. (Top panel) Impedance (Nyquist) plots for bare gold electrode in 3 mM potassium ferrocyanide/potassium ferricyanide in 0.1 M NaF as the supporting electrolyte. (Bottom panel) Impedance (Nyquist) plots of zein deposits on (i) hydrophobic monolayer and (ii) hydrophilic monolayer. The electrolyte used is 3 mM potassium ferrocyanide/ferricyanide in 0.1 M NaF as the supporting electrolyte.

revealing good packing and different arrangement of zein molecules on hydrophilic surfaces. The heterogeneous rate constant values calculated by the procedure reported by Krysinski and Smolska[40] are shown in Table 2. It is clearly observed that the hydrophilic surfaces show lower rate constants than that observed on hydrophobic surfaces due to the highly blocking hydrophilic surface. Impedance measurements have been carried out to follow the charge-transfer resistance for the reaction involving the ferrocyanide/ferricyanide redox couple.[38,41] The Nyquist plot for the bare electrode shows a small semicircle in the high-frequency region followed by a straight line in the low-frequency region oriented at 45°, showing that the process is diffusion-controlled (Figure 4, top). The zein/SAM-modified electrode shows a large semicircle in the entire frequency region [Figure 4 bottom (i, ii)]. The charge-transfer resistance associated with the modified hydrophilic and hydrophobic surfaces are determined to be 7.5×10^4 and 6×10^3 Ω cm^2, and the

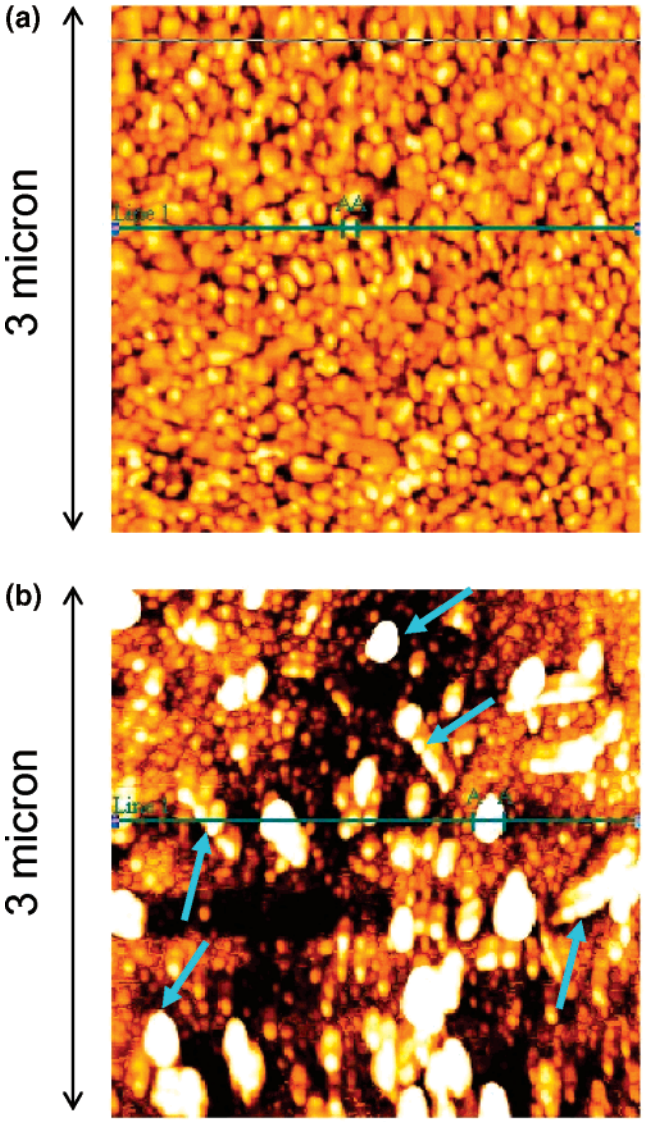

Figure 5. (Top panel) AFM image obtained for zein deposits on undecanethiol monolayer formed on Au(111) surface. Image size is 3×3 μm and scan speed is 1 Hz. (Bottom panel) AFM image obtained for zein deposits on 11-mercaptoundecanethiol monolayer on Au(111) surface. Image size is 3×3 μm and scan speed is 1 Hz.

rate constant values have been determined to be 7.09×10^{-6} and 8.8×10^{-5} cm s^{-1}, respectively.

The barrier property of organic thin films can also be estimated by correlating the defects with impedance parameters[42] from the ac studies. It has been reported that the measurement of phase angle at low frequencies, where the ion diffusion occurs, gives the quality of the thin films in terms of defects and pinholes.[43,44] The phase angle observed for the modified hydrophilic surface is 82°, while the adsorption on the hydrophobic surface shows a phase angle of 73° at 1 Hz frequency (Supporting Information). This substantiates the better adsorption of zein on the hydrophilic surface, with a large number of molecules with smaller defects, compared to the adsorption on hydrophobic surfaces. Zein film on the SAM surface can be thought of as a combination of electrode−SAM and SAM−zein interfaces in series. Hence the capacitance associated with modified surface will be

$$(C_{\mathrm{SAM-zein}})^{-1} = (C_{\mathrm{SAM}})^{-1} + (C_{\mathrm{zein}})^{-1}$$

By knowing the total capacitance of the system from the

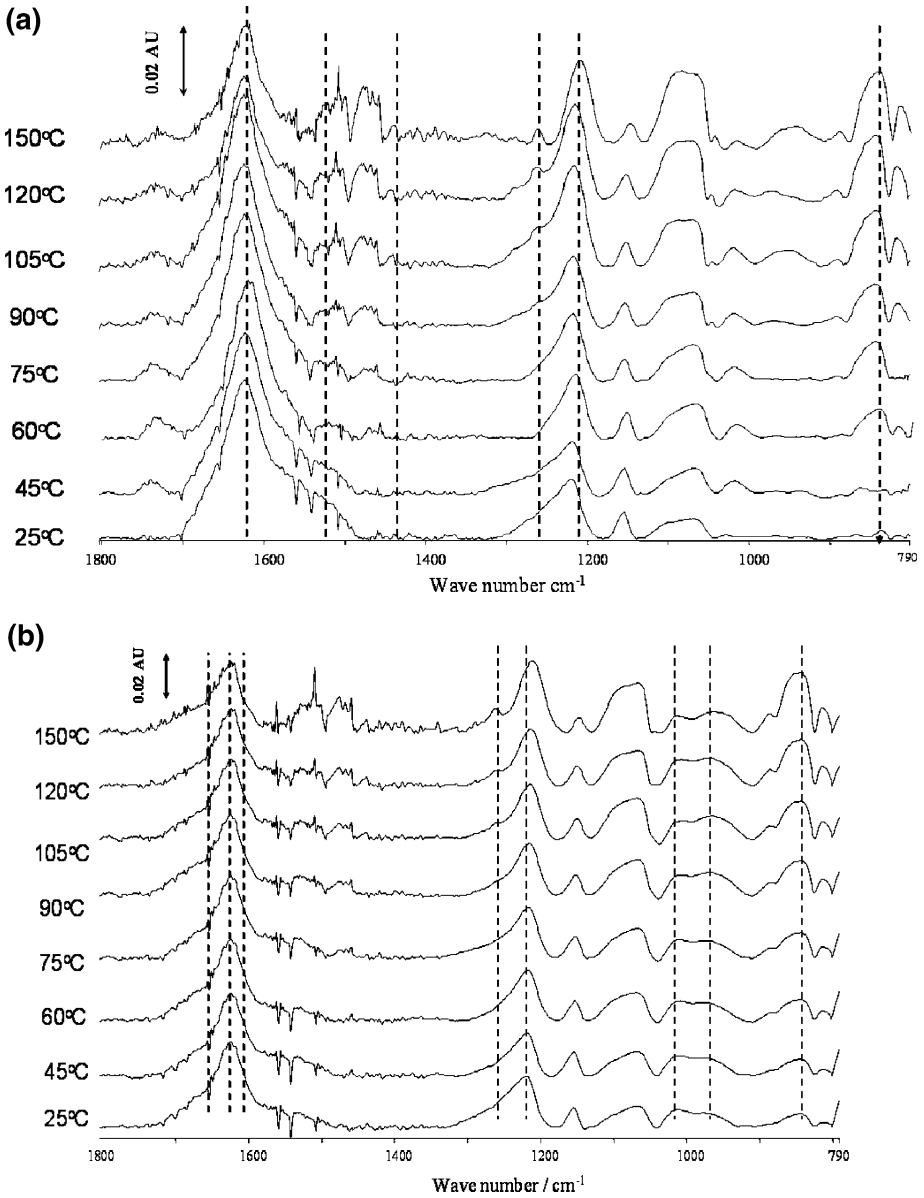

Figure 6. RAIR spectra of zein protein deposits on (top panel) hydrophobic and (bottom panel) hydrophilic surface at various temperatures.

electrochemical measurements and the capacitance value of the SAM (obtained from known parameters for an ordered SAM), it is possible to evaluate the capacitance associated with zein film. The dielectric constant (ϵ) of the zein protein has been calculated to be 22 ± 3. The reported value for the dielectric constant of zein based on conductivity measurements is 32.[45]

Atomic Force Microscopy. Surface topography of zein deposits on hydrophilic and hydrophobic SAMs has been investigated by atomic force microscopy. All images are taken in contact mode with 3×3 μm size in dry state. The roughness of the bare gold surface calculated on the basis of the root-mean-square deviation from the average height is observed to be 1.54 nm (Supporting Information). Au modified with C_{11}-SH SAM (hydrophobic surfaces) shows grains of sizes 150−175 nm, and the average surface roughness is observed to be 4.5 nm. On the other hand, the MuDA-modified Au (hydrophilic surfaces) is relatively smooth with uniform particle distribution and the grain size varies from 55 to 85 nm (Supporting Information) and the surface roughness is observed to be 1.65 nm. After the zein adsorption, the topography of both surfaces changes. The zein deposits on hydrophobic surfaces (Figure 5, top) show uniformly distributed structures and the roughness is observed to be 1.35 nm. This is almost 3 times less than that observed on the base SAM. On the contrary, zein deposits on a hydrophilic surface (Figure 5, bottom) show circular and cylinderlike structures with 25 nm heights. The surface roughness is calculated to be 4.7 nm, which is 3 times higher than the corresponding base monolayer. The topography also shows disc- and wormlike features as indicated by the arrows in Figure 5 (bottom). The features may be the units for the formation of cylinderlike structures with large diameters of 200 nm.[46,47] The tall features stem from the orientation of the zein molecules perpendicular to the surface based on the interaction through the glutamine strands (at the base of the protein). When the adsorption occurs on hydrophobic surfaces, the zein molecules lie flat on the surface with the walls of the cylinders interacting with the SAM. Hence the surface appears to be different. The above results are consistent with the fact that the zein molecule adopts conformational changes that depend on the wettability of the substrate.

Thermal Stability on Hydrophobic Surfaces. The stability of zein deposits under thermal perturbations has been followed by RAIR spectroscopy. The spectra (Figure 6, top) show a

relative decrease in the intensity of the 1622 cm^{-1} band (indicated by dotted lines) due to β structure without any appreciable shift in the wavenumber. This decrease in the intensity may be attributed to the following. As the temperature rises, effective interaction between SAM and zein molecules through the residues in the α-helix structures decreases. This results in the tyrosine and phenylalanine residues coming to the surface from the deeply buried state. This is inferred from the increase in the intensity ratio of bands at 858 and 835 cm^{-1}(indicated by dotted lines). The sharp increase in the intensity of the C−H bending bands around 1455 cm^{-1} also supports the fact that interaction with methyl-terminated SAMs and the functional groups are reduced as the temperature is increased. The protein starts to reorient by refolding toward the nativelike state, that is, α-helix structure.[18] This agrees with the reported results that dissociation of zein aggregates at high temperature increases the α-helix content.[20] The intensity of the band at 1520 cm^{-1} corresponding to β-sheet increases and shifts to low frequencies (1512 cm^{-1}). Correspondingly, the band due to α-helix at 1535 cm^{-1} (as shown by dotted lines) shows an increase in intensity with increasing temperature. This accounts for the dissociation of zein aggregates due to reduced interaction with methyl termini that reorients the protein structure in α-helix form. Hence, as the temperature increases, some fraction of β-sheet structure gets converted into α-helix form. The variation of amide III band clearly shows the conformational changes associated with monolayer orientation. The band at 1222 cm^{-1} shifts to 1210 cm^{-1} (as shown by dotted lines) with a concomitant decrease in the intensity revealing that the β-structure starts to degrade and undergoes conformational changes. Subsequently, the shoulder observed under ambient conditions at 1272 cm^{-1} (as indicated by dotted lines) grows into a clear peak at 1263 cm^{-1}. This corresponds to the formation of α-helix structure in zein.

Hydrophilic Surfaces. Conformational changes associated with the zein deposits are different in the case of hydrophilic surfaces (Figure 6, bottom). The amide I band at 1622 cm^{-1} decreases in intensity and shifts to low frequencies, showing that there occurs a reorientation of the β-structure. But the decrease in intensity is small when compared to the intensity variation observed on hydrophobic surfaces. The band related to α-helix structure is observed as a shoulder at 1661 cm^{-1} under ambient conditions, indicating that an appreciable amount of α-helix structure is present in the deposits. This emphasizes the effect of surface wettability on the conformation changes associated with the adsorbed protein. As the temperature increases, the band at 1622 cm^{-1} starts to develop as a shoulder at 1604 cm^{-1}, bringing out the presence of free glutamine turns and thus implying reduced interaction of zein with the SAMs. The band related to the α-helix structure is observed as shoulder at 1661 cm^{-1} at temperatures above 90 °C and is a clear indication of the facile transformation of α-helix structure at the expense of already existing β-sheet structure. This band is not observed in the case of zein deposits on hydrophobic surfaces. The amide III band also confirms this trend. The band at 1220 cm^{-1} under ambient conditions for β-structure is reduced in intensity as the temperature is increased. Accordingly, the band at 1262 cm^{-1} attributed to the α-helix structure increases monotonically after about 120 °C. The refolding of zein protein to nativelike α-helix structure is supported by the substantial increase in the intensity of the band for free tyrosine and phenylalanine residues (840, 868, 974, and 1007 cm^{-1}) that are responsible for folding to α-helix structure. By and large, the adsorption of zein on hydrophobic as well as hydrophilic surfaces leads to denaturation accompanied by the transformation of α-helix to β-sheet structure. The stability of the zein deposits is found to be good on the basis of few changes observed in the RAIR spectrum after 1 week of adsorption.

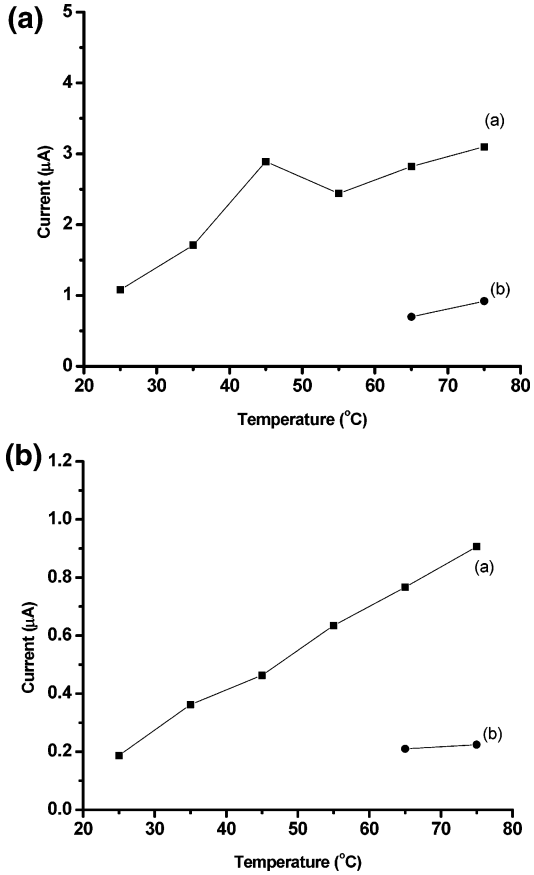

Figure 7. (Top panel) Temperature dependence of currents for zein deposits on hydrophilic SAM-modified electrode (a) observed in the presence of 5 mM potassium ferrocyanide/ferricyanide and 0.1 M NaF as the supporting electrolyte. The points on curve b show the data at room temperature after cooling the system was cooled from the corresponding high temperature shown on the $-x$-axis. The solid lines are only guidelines to the eye. (Bottom panel) Temperature dependence of currents for zein deposits on hydrophobic SAM-modified electrode (a) observed in the presence of 5 mM potassium ferrocyanide/ferricyanide and 0.1 M NaF as the supporting electrolyte. The points on curve b show the data at room temperature after the system is cooled from the corrresponding high temperature shown on the $-x$-axis. The solid lines are only guidelines to the eye.

Thermal Stability of Zein Deposits on SAMs in Wet Conditions. Electrochemical measurements based on the blocking behavior of the SAMs assert the quality and order of the zein-based films, and this property has been used to follow the defects introduced by temperature perturbations. Figure 7 (top) shows the plot of current density (at the formal potential of $[Fe(CN)_6]^{4-/3-}$, 0.2 V) versus temperature for the zein protein adsorbed on hydrophobic SAM-modified gold electrode prepared from undecanethiol. As the temperature is increased, a steady increase in the current density is observed, revealing that the packing becomes less dense as a function of temperature. Another point to be noted here is that the protein arrangement on SAM surface is reversed when the temperature is brought back to 25 °C. The points on curve b show the current density measured at 25 °C after an increase in the corresponding temperature shown on the x-axis. It is clear from the figure that even after the monolayer is heated up to 75 °C, the current density returns to the original value observed under ambient

conditions. Similar behavior (Figure 7, bottom) is observed for zein films adsorbed on SAMs prepared from mercaptoundecanoic acid except that the current density is lower than that observed in the former case. Here again the protein arrangement is reversed when the temperature is brought back to 25 °C after thermal perturbations. The rate constant values (Table 2) increase with increasing temperature for both the deposits with the values 1 order higher on hydrophobic surfaces as compared to the film on hydrophilic surfaces. This clearly brings out the high affinity of zein for hydrophilic surfaces, leading to a compact arrangement with high surface coverage and stability. The structure of zein after adsorption on hydrophilic monolayer comparatively does not get altered much and the structure is conformationaly stable.

Summary. Zein shows better affinity toward hydrophilic surfaces than hydrophobic surfaces. The RAIR studies show the conformation changes of the protein leading to denaturation under ambient conditions. The adsorption modes and conformational changes are different for hydrophilic and hydrophobic surfaces. Thermal perturbations in the dry state induce refolding of the protein structure toward nativelike state. Under wet conditions, the zein deposits are stable and show reversibility of conformational changes as a function of temperature. The zein molecule adopts close to a perpendicular orientation on a hydrophilic surface, while on a hydrophobic surface it seems to be almost flat. The studies described here may open up possibilities of using zein as a protective, impermeable coating for food packaging, wherein different conditions such as hydrophilic and hydrophobic surfaces may be required to store edible materials.

Acknowledgment. We thank the DST and CSIR, New Delhi, for financial assistance.

Supporting Information Available. FT-IR spectrum of bulk zein protein; Bode-phase angle plot for zein deposited on hydrophobic and hydrophilic monolayers on gold in 0.1 M NaF; AFM images obtained for a Au(111) surface on mica, and undecanethiol and 11-mercaptoundecanethiol monolayers on Au(111) surfaces. This material is available free of charge via the Internet at http://pubs.acs.org.

References and Notes

(1) Sigal, G. B.; Mrksich, M.; Whitesides, G. M. *J. Am. Chem. Soc*. **1998**, *120*, 3464.
(2) Jenkins, S. H.; Heineman, W. R.; Halsall, H. B. *Anal. Biochem.* **1988**, *168*, 292.
(3) Kessler, G. H.; Lund, D. B. In Kessler, G. H., Lund, D. B., Eds.; Prien Chiemsee, 1989.
(4) Baier, R. E.; Meyer, A. E.; Natiella, J. R.; Natiella, R. R.; Carter, J. M. *J. Biomed. Mater. Res.* **1984**, *18*, 337.
(5) Silin, V.; Weetall, H.; Vanderah, D. *J. Colloid Interface Sci*. **1997**, *185*, 94.
(6) Wertz, C. F.; Santore, M. M. *Langmuir* **1999**, *15*, 8884.
(7) Wertz, C. F.; Santore, M. M. *Langmuir* **2001**, *17*, 3006.
(8) Haynes, C. A.; Norde, W. *Colloids Surf. B: Biointerfaces* **1994**, *2*, 517.
(9) Schakenraad, J. M.; Busscher, H. J. *J. Colloids Surf.* **1989**, *42*, 331.
(10) Iwami, K.; Hattori, M.; Nakatani, S.; Ibuki, F. *Agric. Biol. Chem.* **1987**, *51*, 3301.
(11) Iwami, K.; Hattori, M.; Ibuki, F. *J. Agric. Food Chem.* **1987**, *35*, 628.
(12) Di Gioia, L.; Guilbert, S. *J. Agric. Food Chem*. **1999**, *47*, 1254.
(13) Gennadios, A.; Weller, C. L. *Food Technol*. **1990**, *44*, 63.
(14) Pomes, A. F. In *Encyclopedia of Polymer Science and Technology*; Mark, H., Ed.; Wiley: New York, 1971; Vol. 15, pp 125.
(15) Matsushima, N.; Danno, G. I.; Takezawa, H.; Izumi, Y. *Biochim. Biophys. Acta* **1997**, *1339*, 14.
(16) Wang, Y.; Rakotonirainy, A. M.; Padua, G. W. *Starch* **2003**, *55*, 25.
(17) Mrksich, M.; Sigal, G. B.; Whitesides, G. M. *Langmuir* **1995**, *1*, 4383.
(18) Mizutani, Y.; Matsumura, Y.; Imamura, K.; Nakanishi, K.; Mori, T. *J. Agric. Food Chem.* **2003**, *51*, 229.
(19) Wang, J. Y.; Miyazawa, T.; Fujimoto, K. *Agric. Biol. Chem.* **1991**, *55*, 1531.
(20) Matsumura, Y.; Murakami, H.; Mori, T. *J. Agric. Food Chem.* **2004**, *52*, 3570;
(21) Li-Chan, E. C. Y. *Trends Food Sci. Technol.* **1996**, *7*, 361.
(22) Hsu, B. L.; Weng, Y-M.; Liao, Y-H.; Chen, W. *J. Agric. Food Chem*. **2005**, *53*, 5089.
(23) Belitz, H.-D.; Kieffer, R.; Seilmeier, W.; Wieser, H. *Cereal Chem.* **1986**, *63*, 336
(24) Choi, K.-H.; Friedt, J.-M.; Frederix, F.; Campitelli, A.; Borghs, G. *Appl. Phys. Lett.* **2002**, *81* (7), 1335.
(25) Kawaguchi, T.; Yasuda, H. K; Shimazu, K. *Langmuir* **2000**, *16*, 9830.
(26) Muthuselvi, L.; Dhathathreyan, A. *Pramana* **2006**, *66* (*3*), 563.
(27) Wilson, C. M. *Cereal Chem.* **1988**, *65*, 72.
(28) Sauerbrey, G. Z. *Z. Phys* **1959**, *155*, 206.
(29) Wang, Q.; Wang, J.-F.; Geil, P. H.; Padua, G. W. *Biomacromolecules* **2004**, *5*, 1356.
(30) Kretschmer, C. B. *J. Phys. Chem.* **1957**, *61*, 1627.
(31) Fraser, R. D. B. *J. Chem. Phys.* **1956**, *24*, 89.
(32) Ambrose, E. J.; Elliott, A. *Proc. R. Soc. London* **1951**, *A208*, 75.
(33) Argos, P.; Pederson, K.; Marks, M. D.; Larkins, B. A. *J. Biol. Chem.* 1982, *257*, 9984.
(34) Tatham, A. S.; Field, J. M.; Morris, V. J.; Anson, K. J. I.; Cardle, L.; Dufton, M. J.; Shewry, P. R. *J. Biol. Chem.* **1993**, *268*, 2625.
(35) Miyarawa, T.; Shimanouchi, T.; Mizushima, S. *J. Chem. Phys.* **1956**, *24*, 408.
(36) Becka, A. M.; Miller, C. J. *J. Phys. Chem.* **1992**, *96*, 2657.
(37) Finklea, H. O.; Hanshew, D. D. *J. Am. Chem. Soc.* **1992**, *114*, 3173.
(38) Katz, E.; Willner, I. *Electroanalysis* **2003**, *15*, 913.
(39) Finklea, H. O.; Snyder, D.; Fedyk, A. J.; Sabatani, E.; Gafni, Y.; Rubinstein, I. *Langmuir* **1993**, *9*, 3660.
(40) Krysinski, M.; Smolska, B. *J. Electroanal. Chem* **1997**, *424*, 61.
(41) Ganesh, V.; Lakshminarayanan, V. *Langmuir* **2006**, *22*, 1561.
(42) Protsailo, L. V.; Fawcett, R. W. *Langmuir* **2002**, *18*, 8933.
(43) (a) Boubour, E.; Lennox, R. B. *Langmuir* **2000**, *16*, 4222. (b) Boubour, E.; Lennox, R. B. *Langmuir* **2000**, *16*, 7464.
(44) Boubour, E.; Lennox, R. B. *J. Phys. Chem. B* **2000**, *104*, 9004.
(45) Wyman, J., Jr. *J. Biol. Chem*. **1931**, *90*, 443.
(46) Wang, Q.; Crofts, A. R.; Padua, G. W. *J. Agric. Food Chem.* **2003**, *51* (25), 7439
(47) Guo, Y.; Liu, Z.; An, H.; Li, M.; Hu, J. *J. Cereal Sci.* **2005**, *41*, 277.

BM0701999